1993 – 17

RADON SOURCES AND EMANATION IN GRANITIC SOIL AND SAPROLITE

Harold Wollenberg and Steve Flexser
Lawrence Berkeley Laboratory
Berkeley,CA

George Brimhall and Chris Lewis
University of California
Berkeley,CA

ABSTRACT

Petrological and geochemical examinations of soil, saprolite, and quartz diorite protolith have been made at the Small Structures field site, Ben Lomond Mountain, California. Variations in Ra in soil and saprolite are mainly controlled by heterogeneities inherited from the parent quartz diorite. Fission-track radiography shows that U is concentrated in the primary accessory minerals, zircon and sphene. However, most importantly for Rn emanation, U is also concentrated in secondary sites: weathered sphene, biotite and plagioclase, grain coatings, and Fe-rich fracture linings which also contain a rare-earth phosphate mineral. This occurrence of U along permeable fracture zones suggests that soil-gas Rn from depth (>2m) is a significant contributor to Rn availability near the surface. Zones highest in emanation occur where fine pedogenic phases: gibbsite, amorphous silica, and iron oxyhydroxide are most abundant. Mass balance analyses of this soil-saprolite profile are in progress and preliminarily indicate that a high-emanation zone corresponds to the upper portion of a zone of accumulation of U and Ba.

INTRODUCTION

To better understand the sources of radon and its availability for transport through the soil, the ingress of Rn into the basements of houses is being investigated in "mini-basement" structures installed in the shallow sub-surface. At this "small structures" installation, the movement of Rn from its sites in the soil, through the soil-pore system and, by way of controlled entry slots, into the basements is examined in detail.(Fisk et al., 1992). For complete characterization of the site and to understand the source of the Rn, the distribution of U and Ra in soil and bedrock were investigated (Flexser et al., 1993). Samples were obtained mainly from core and auger holes, with additional samples from outcrops and soil rock fragments. Radioelement contents and radon emanation rates of bulk samples were determined by gamma-spectrometry, complemented by microscopic examination of fission-track radiographs of grain mounts and polished thin sections, and by electron microscopy (SEM) with x-ray spectroscopy (EDS) to obtain compositional data. Clay mineral contents were also characterized by x-ray diffraction, and soil solutions of 1:1 soil:water mixtures were obtained and analysed by ICP-Atomic Emission Spectroscopy.

SITE AND SOIL CHARACTERISTICS

The Small Structures site is located on Ben Lomond Mountain, CA, a 790 m-high broad-topped ridge (Fig. 1), with high seasonal rainfall (~150 cm per year), occurring mainly during the period October - May. There is occasionally light snowfall, but the ground does not freeze. The topography and climate have encouraged deep weathering of the granitic bedrock, forming a well-developed saprolite to >5 m Near the surface, a brown sandy loam is present to depths between 1.4 and 2.4 m, overlying the saprolite across an irregular and partly transitional boundary. Roots and burrow holes are very abundant to depths of >3 m. The soil parent rock or protolith is weathered quartz diorite of the Ben Lomond pluton (Bowman and Estrada, 1980; Leo, 1967), a medium-grained granitic rock containing abundant finer- and coarser-grained inclusions and dikes. The main mineral constituents of the quartz diorite are plagioclase, quartz, potassium feldspar, biotite, and hornblende; accessory minerals include sphene, zircon, ilmentite, epidote, apatite, and minor monazite and allanite. Most minerals, particularly biotite and plagioclase, show significant effects of weathering, with quartz and zircon the only minerals consistently clear and unweathered. Clay-size gibbsite($AlOH_3$) and kaolinite or halloysite(Al-OH silicates), occur as weathering products.

Mineralogically, the main difference between the soil and the weathered protolith is the abundance of gibbsite, which occurs in the soil from the surface through the upper saprolite (to ~2.5 to 3 m depth). Smectite, by contrast is abundant in the soil only below the upper saprolite. The deeper saprolite is distinctly more intact than the upper saprolite, and protolith igneous textures are well preserved. The deeper saprolite also maintains abundant narrow, near-vertical fractures consisting of zones ~5 mm wide (Fig. 2), darkly stained and coated by Fe-oxyhydroxide (Fe-OOH) and possibly organic matter, and bordered by deformed and fragmented mineral grains. Fine root casts are present in the fracture zones to depths of at least 5 m.

RADIOELEMENT DISTRIBUTION

The abundance and distribution of radioelements were determined on bulk and microscopic scales. Bulk-scale analyses employed gamma-spectrometry for Ra (direct precursor of Rn), Th, and K, and for determination of Rn emanation rates. Results of analyses of bulk soil and rock samples are shown in Figure 3, which combines data from soil samples from a core hole (C) and an auger hole (A), as well as grab samples from the two structure excavations, and rock samples from soil and outcrop. Soil Ra concentrations vary between 0.61 and 1.33 pCi g^{-1}, corresponding to 1.71 and 3.76 ppm equivalent U (based on U-series secular equilibrium, and corrected for Rn emanation). Most of the variation in radioelement concentrations (Fig. 3B-D) is attributable to heterogeneities inherited from the parent granitic rock rather than to secondary radioelement redistribution by pedogenic processes. This is suggested by the contrasting radioelement contents of rock samples X and Z, texturally and mineralogically distinct phases of the parent rock, compared with the main phase of weathered quartz diorite (sample Q_2). It is also indicated in the anomalously high radioelement concentrations of the auger (A) samples between 80 and 120 cm depth, which contain abundant rock fragments very similar to sample X. Aside from this anomalous interval (and that at 330 cm in core C, also likely due to parent rock heterogeneity), the auger and core samples' radioelement contents match reasonably well, as do those from the east excavation; a poorer match is observed with the samples from the west excavation.

Rn emanation rates (Fig. 3A) show a pattern of variation apparently independent of that of the radioelement concentrations, and related instead to soil zonation (Fig. 3, left side): emanation increases with depth through the upper loam, peaks in the transitional soil zone and upper saprolite, and returns to a rather constant lower level in underlying saprolite. The variation shown by Rn emanation also is similar to the variation observed in the abundance of fine pedogenic phases, notably gibbsite, in the soil, as discussed below. The large differences in emanation rates of the three rock samples reflects different degrees of weathering and redistribution of U (and Ra) on accessible grain boundaries and secondary minerals.

On the microscopic scale, the distribution of U in soil and parent rock was investigated by fission-track radiography to provide a guide to Ra distribution. U in the soil is located in: 1) small granitic accessory minerals, predominantly zircon; 2) primary igneous minerals weathered partly or completely, most frequently sphene; 3) margins and cracks in mineral grains; and 4) fracture zones in the saprolite. Secondary sites (2, 3, 4 above), which show prior mobilization of U in the soil or parent rock, are the main focus here, as U and Ra concentrate more readily on grain boundaries and pore walls at these sites, enabling recoiling Rn atoms to emanate much more readily than from primary minerals. Table 1 summarizes the sites of elevated U concentration in the soil and rock samples. Sphene is the most common site, containing widely varying U concentrations usually ranging between 100 and 400 ppm, but with both lower and higher concentrations (to ≥700 ppm) also common. Mineral grain-boundary coatings also commonly contain U (Fig. 4), with more-uraniferous sites ranging between 20 and 200 ppm U, and in some cases to ≥700 ppm (Table 1). Less commonly, significant U is associated with weathered plagioclase or biotite, and occasionally with epidote, allanite or apatite. Also, minute highly uraniferous grains of uraninite and monazite are sometimes observed, usually enclosed within primary biotite or feldspar crystals.

Compositional data for the main types of U-bearing sites in the soil and parent rock show that U enrichment in secondary sites generally corresponds with very high Ti concentrations (to ≥70% TiO_2), along with elevated Al, Fe, and P contents, with more-mobile elements like Ca and K removed by solution. Weathering in primary minerals, especially sphene and biotite, is characterized by a porous, skeletal or mesh-like framework on which Ti is concentrated, with recesses in the framework containing high concentrations of Al. U-bearing grain-boundary coatings contain minute (sub-micron) grains of rutile or anatase, as well as Th- and REE-bearing phases. In samples of parent rock, large differences in U concentration were observed between weathered and unweathered sphene;

similar differences were not noted in soil samples, suggesting that U is fixed temporarily in residual weathered sphene in the soil protolith, and later remobilized during further weathering in the soil.

In the saprolite, U is consistently present at elevated levels in the steeply dipping fracture zones, where it is associated with Fe-OOH, and locally with a secondary REE-phosphate mineral. Figure 4 illustrates textural features and U associations of the fracture zones examined in intact polished sections. U concentrations in the dense Fe-rich fracture coatings generally vary between ~20 and 90 ppm U, averaging 30-50 ppm (Table 1), while in the phosphate mineral they average 5 to 10 times higher (200 to >580 ppm).

A mass balance analysis of the Ben Lomond soil profile, using the methodology of Brimhall et al (1992) is in progress, and shows that the soil-saprolite transition is the upper boundary of U accumulation, occurring below a zone of U depletion in the shallow soil. In this methodology, absolute mass changes due to transport of an element ("delta U" in Fig. 5) are based on the volume change of the soil determined from Zr concentrations (zircon exhibits essentially no weathering) and bulk sample densities. The U accumulation with depth corresponds generally with accumulations of Ba, Al, Si, and Fe in the depth range 2.2 -2.6 m., in keeping with the aforementioned mineralogical associations. The U-Ba correspondence suggests that U and its Ra daughter are not separated, as also indicated by high-resolution gamma spectrometry, which shows secular equilibrium between U and Ra.

DISCUSSION

The observed preferential distribution of U on secondary sites - grain boundaries, fractures, and relatively porous weathered minerals - is reflected in the high Rn emanation rates (between ~30% and 50%) of the Ben Lomond soil. However, the detailed variation in Rn emanation with depth is not readily explained by variation in U distribution. Highest emanation rates occur between 1.3 and 2.3 m depth (Fig. 3A), and in this interval soil clay fractions show a maximum in the relative abundance of gibbsite, the main crystalline pedogenic phase, as well as abundant amorphous silica and Fe-OOH. This suggests that enhanced emanation is related to the occurrence of these pedogenic phases.

Further insight into pedogenic processes was provided by chemical analyses of soil solutions, which served as guides to which elements are most readily released to solution in the soil and saprolite. Compositional data on the soil solutions show that numerous elements are relatively abundant in the shallow soil but decline sharply below. Most notable are Al, Ti, and Fe, which figure prominently in secondary U-bearing sites, and which follow very similar patterns with depth in the soil solutions. The presence in solution of these elements - particularly Al and Ti, which are highly immobile in most geochemical environments - in the upper 1-1.5 m of the soil indicates that shallow soil fluids are quite acidic due to abundant rainfall and vegetation, and are possibly locally reducing. These elements (as well as others soluble only in the topmost soil) probably precipitate in this shallow soil or at adjacent depths as hydroxides or hydrous oxides; the concentration of gibbsite, silica, and Fe-OOH observed between 1.3 and ≥2 m depth indicates that a portion of these precipitated phases are then transported by suspension in soil fluids and accumulate in this depth interval. Sorption of radionuclides by these colloidal phases (and possibly also by colloidal organic matter) probably explains the high Rn emanation rates observed in this interval. This conclusion is broadly consistent with modeling by Semkow (1990) of Rn emanation rates from particulate matter on which Ra is distributed preferentially on surficial coatings. The high emanation rates in this soil interval could readily result, by this model, from sorption of Ra onto colloidal particles in the size range observed in soil clay suspensions (abundant at ≥0.3 μm), given their likely formation by aggregation of finer precipitates.

CONCLUSIONS

Secondary sites of U are most important to Rn generation and emanation. The main U associations are with weathered sphene, grain boundary coatings, and weathered biotite and plagioclase. Enhanced concentrations of Ti, Al, Fe, and/or P are usually present where U is concentrated in secondary sites. U is also present in significant concentrations in Fe-rich fracture coatings in the saprolite, and in a phosphate mineral and Ti-rich grain coatings in fracture zones.

High Rn emanation occurs in a depth interval where gibbsite, the main crystalline pedogenic phase, shows a marked increase in abundance, and amorphous silica and Fe-OOH are also prominent.These generally coincide with

a zone where mass balance analysis indicates an accumulation of U and Ba. Colloidal precipitates of Al, Fe, Ti, Mn, and other elements which are mobile in the upper ~1 m of soil are transported and accumulate at these depths. High emanation there is consistent with sorption of U on colloidal surfaces.

ACKNOWLEDGEMENTS

Andy Yee, LBL analyzed soil solution samples, and Ron Wilson of the Department of Material Science and Mineral Engineering, U. C. Berkeley, assisted with electron microscopy. Thermal neutron irradiations were provided by the Oregon State University Radiation Center. We thank Harold Wells and his staff at the California Division of Forestry's Ben Lomond Nursery for their cooperation and support at the field site. This work was supported by the Director, Office of Energy Research, Office of Health and Environmental Research, Environmental Sciences Division of the U.S. Department of Energy, under contract DE-AC03-76SF00098.

REFERENCES

Bowman, R. H., and Estrada, D.C. Soil survey of Santa Cruz County, California. U.S. Department of Agriculture, Soil Conservation Service; 1980.

Brimhall, G., Chadwick, O., Lewis, C., Compston, W., Williams, I., Danti, K., Dietrich, W., Power, M., Hendricks, D., and B att, J. Deformational mass transport and invasive processes in soil evolution. *Science* 255: 695-702;1992.

Flexser, S., Wollenberg, H., and Smith, A. Distribution of radon sources and effects on radon emanation in granitic soil at Ben Lomond, California. *Environmental Geology*, in press; 1993.

Fisk, W.J., Modera, M.P., Sextro, R.G., Garbesi, K., Wollenberg, H.A., Narasimhan, T.N., Nuzum, T., and Tsang, Y.W. Radon entry into basements: approach, experimental structures, and instrumentation of the small structures research project. Lawrence Berkeley Lab. Rept. LBL-31864;1992.

Leo, G.W. The plutonic and metamorphic rocks of the Ben Lomond Mountain area, Santa Cruz County, California. Calif. Div. Mines Geol. Spec. Rept. 91: 27-43; 1967.

Semkow, T.M., 1990. Recoil-emanation theory applied to radon release from mineral grains. *Geochim. Cosmochim. Acta* 54: 425-440; 1990.

Table 1. Sampling of representative U-bearing sites in soil and parent rock.

U site type	[a]sample	#	mean U (ppm)	(±s. d.)	[b]range (ppm)	comments
sphene	76-91	15	252	(±145)	91-590	
	128	8	251	(±199)	77->700	186 (±81) ppm without outlier
	152-168	34	181	(±115)	30->420	
	195	5	102	(±52)	30-190	
	247-317	6	98	(±65)	53-220	
	497	5	209	(±112)	84-340	
	Q_1	10	157	(±186)	39->630	105 (±92) ppm without outlier
	X	17	274	(±139)	40-550	
	Y	8	361	(±211)	86-630	very high U concentrations in altered sphene not included
grain boundaries	76-91	6	231	(±228)	56->660	144 (±90) ppm without outlier
	128	4	>30	(±9)	20->40	
	195	1	>22			
	247	4	120	(±117)	42-290	62 (±19) ppm without outlier
	Q_1	1	134			
	X	2	>87		44->130	
altered biotite	76-91	1	84			
	195	2	58		21-95	
	247	2	51		37-65	
	Q_2	1	149			
altered plagioclase	76-91	3	76	(±81)	17-160	
	Y	3	48	(±17)	37-68	
epidote	128	1	250			
	152-168	1	56			
	317	1	51			
	X	1	60			
	Y	1	38			
	Q_1	2	>47		35->58	
altered allanite	X	6	159	(±83)	82-320	
	Y	1	>440			
apatite	Q_1	3	253	(±324)	64-630	66 (±3) ppm w/o outlier
fractures in saprolite	317	2	195		180-210	maximum, assoc. with phosphate
	317	3	33	(±18)	20-55	typical Fe-rich fractures
	497	2	390		210-≥580	maximum, assoc. with phosphate
	497	4	57	(±25)	33-90	typical Fe-rich fractures
	497	3	284	(±69)	200-340	grain coatings

[a] depths (cm) for soil samples; rock samples designated by:
Q_1 - relatively unweathered quartz diorite, outcrop.
Q_2 - very weathered quartz diorite, soil clast.
X - coarse-grained light-colored dike or inclusion, soil clast.
Y - medium-grained dark granitic inclusion, soil clast

[b] minimum concentrations given where high fission-track density, small grain size, or linear site geometry preclude reliable estimation of U content.

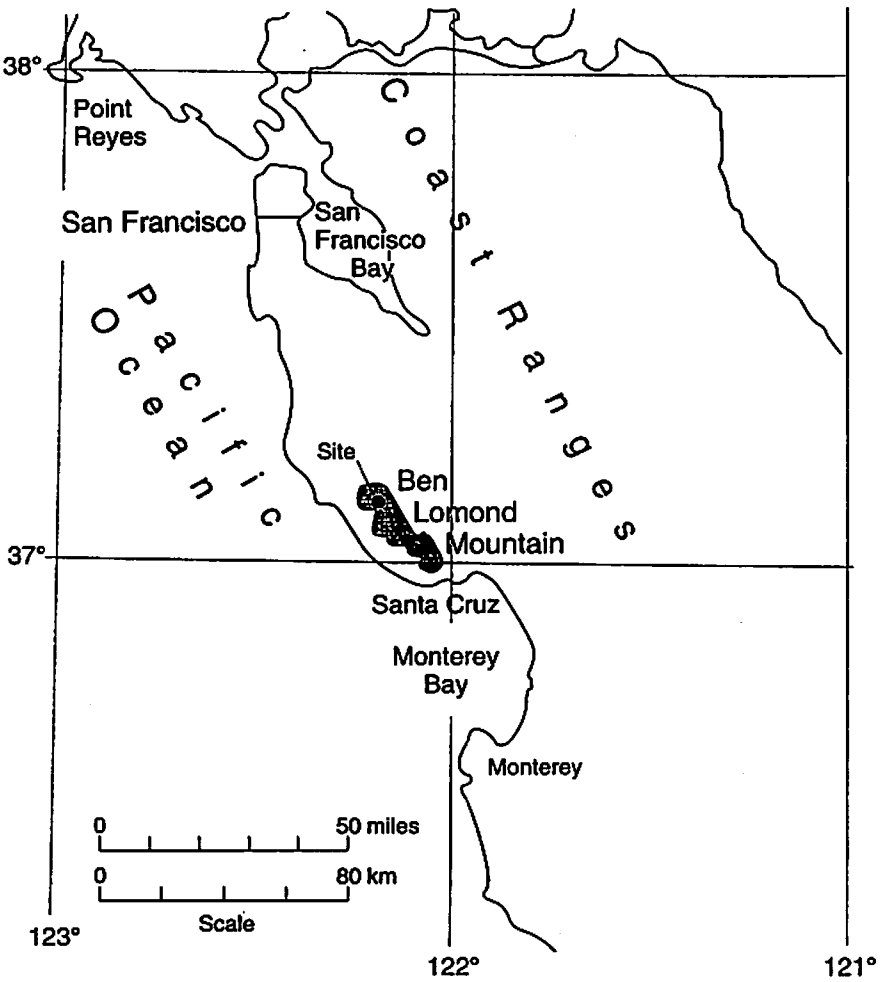

Fig. 1. Location map showing Small Structures site on Ben Lomond Mt., north of Santa Cruz, California.

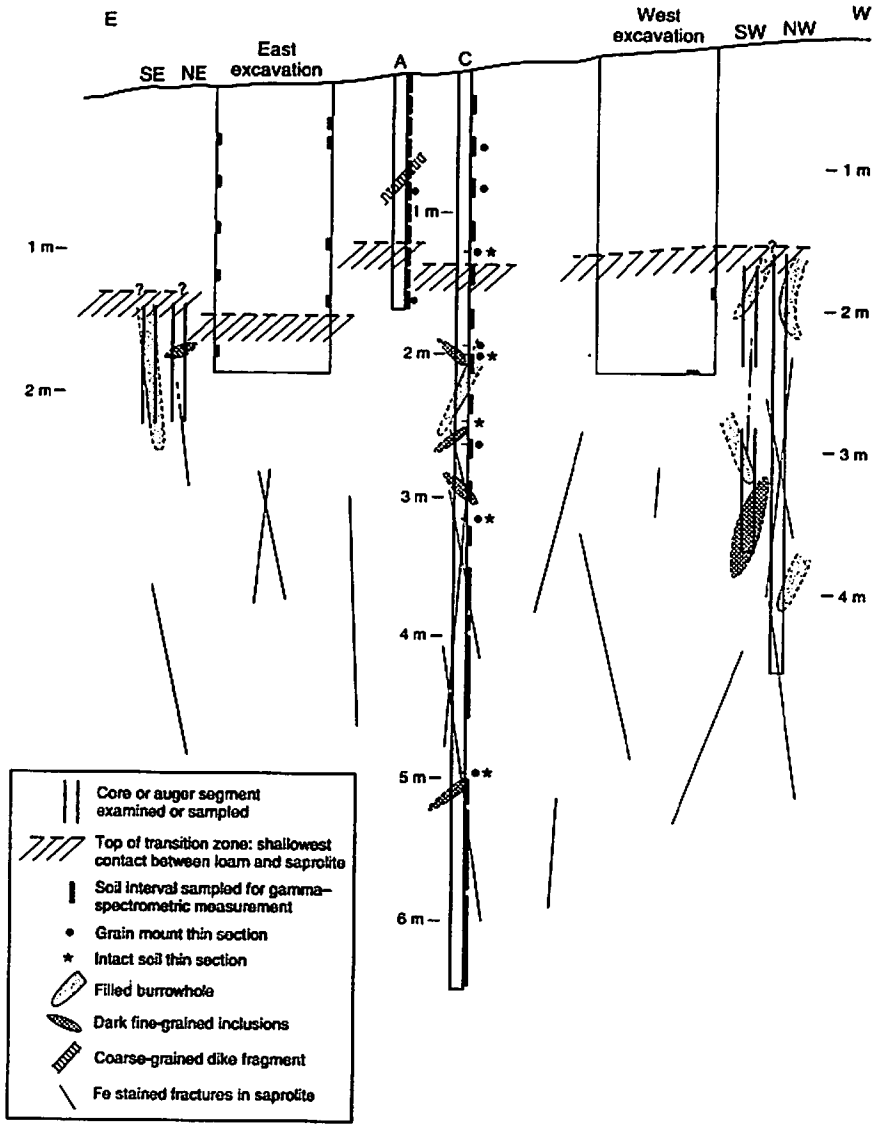

Fig. 2. Schematic cross section through radon field site. Depths along core and auger holes are accurate, but lateral relationships are schematic. Fractures are shown where observed in cores, and pictorially elsewhere.

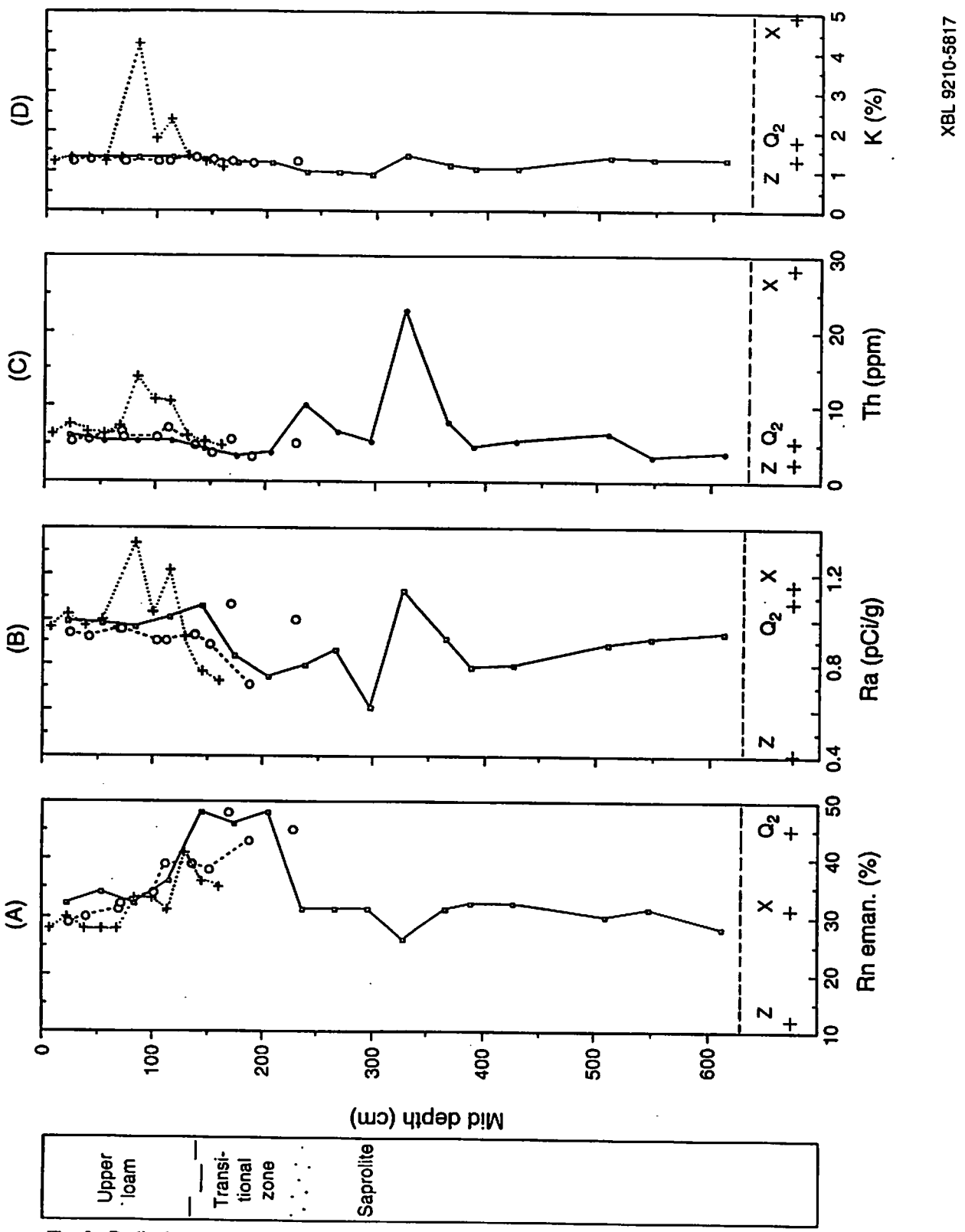

Fig. 3. Radioelement concentrations and radon emanation rates of samples from core hole (solid line), auger hole (dotted line, crosses), and walls and floor of excavations (circles). Q2, X and Z represent intact rock samples of weathered quartz diorite, coarse-grained dike fragment, and a fine-grained dark inclusion, respectively.

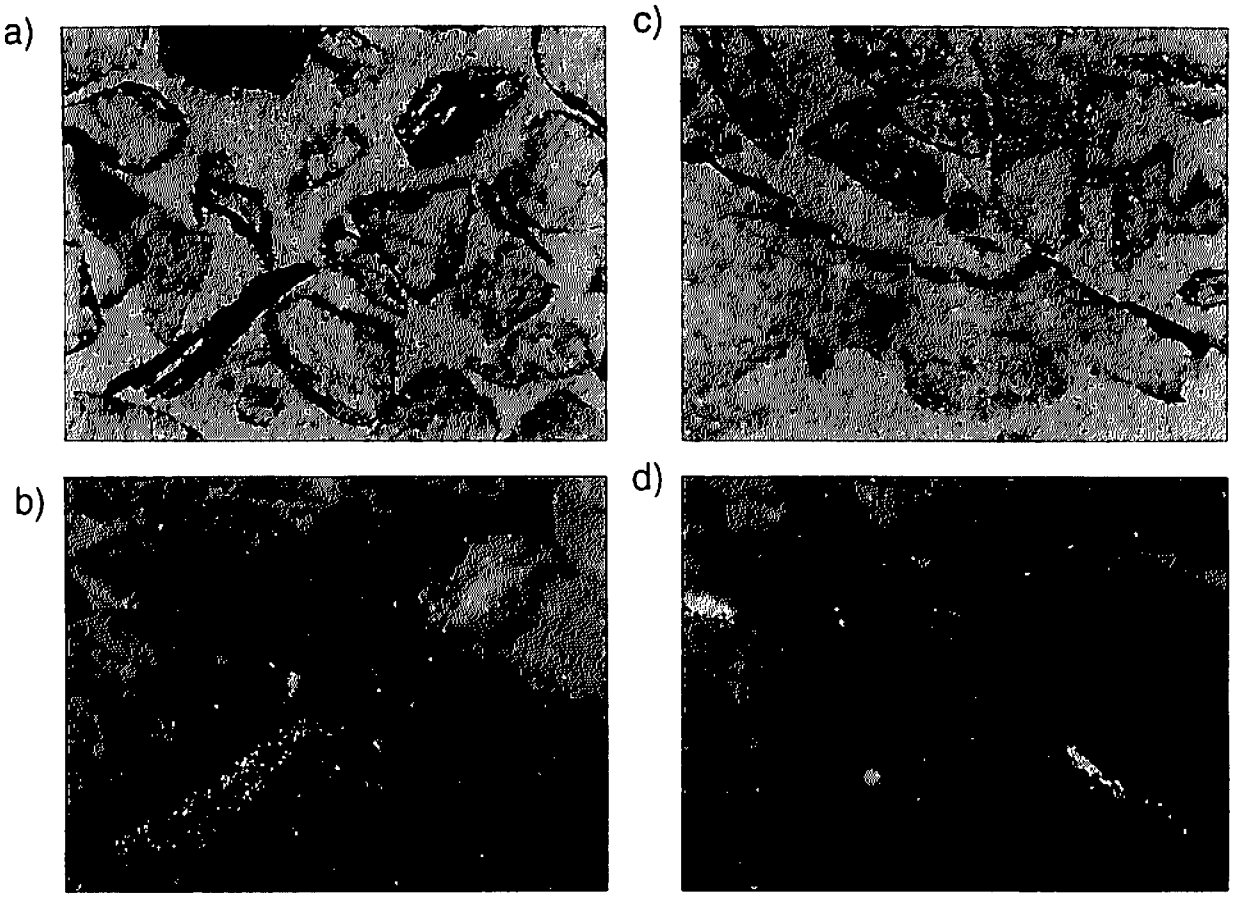

Fig. 4. Uraniferous grain boundary coatings and associated fission tracks, from 76-91 cm depth. Edges and cleavage traces in biotite-vermiculite at lower left in (a) and (b) contain >170 ppm U, and Fe-rich coating and cementation of quartz grain at upper right contains ~70 ppm. Dark edges of large fractured quartz grain in (c) are chlorite containing ~20 ppm ((d), lower right) and 300 to >600 ppm ((d), upper left) where Ti-rich inclusions are present. All frames are 1.8 mm across.

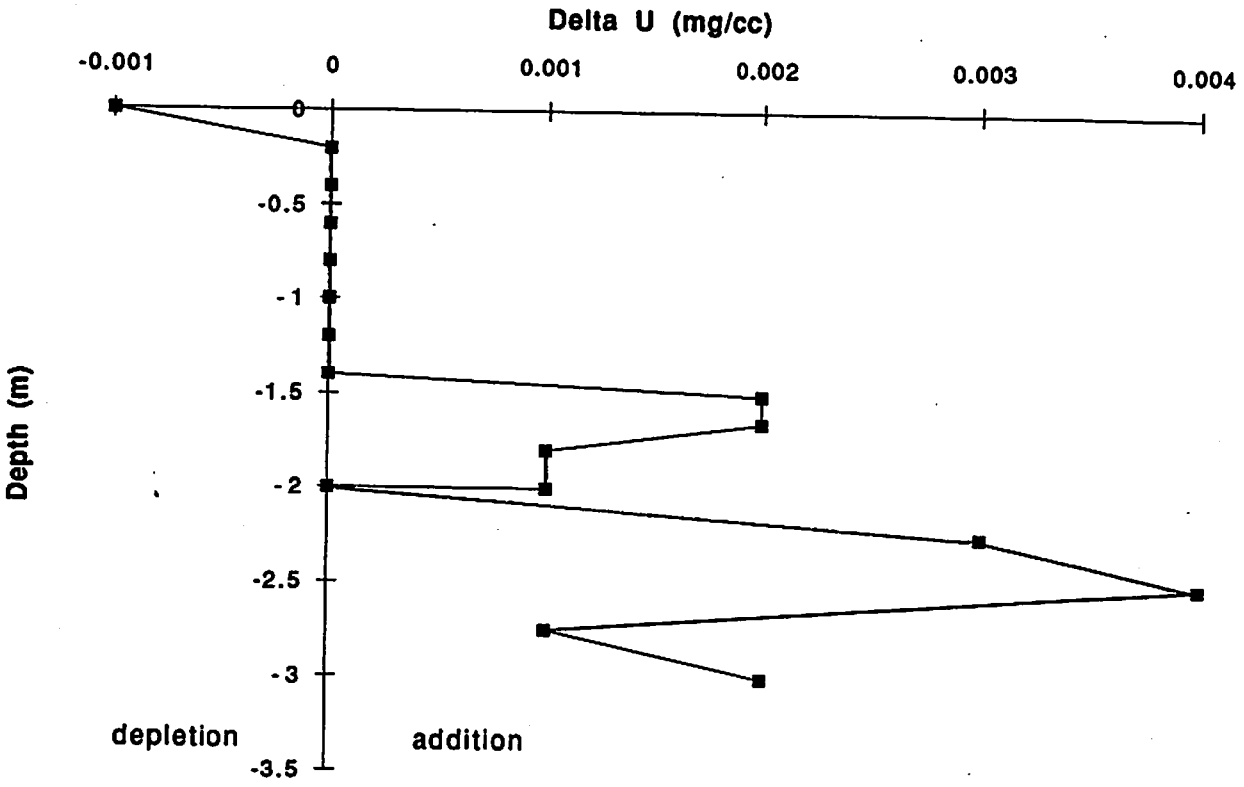

Fig. 5. Mass changes due to transport of U, based on volume change determined from Zr concentrations and bulk sample densities (Brimhall et al., 1992). Negative value indicates depletion of mass, zero indicates residual retention, and positive values indicate introduction of mass.